JAG1-Notch signaling drives M1 macrophage polarization in osteoarthritis

Shufeng Yang[1], Li Jiao[1], Chengcheng Jiang[1], Guang Li[2]*, Fan Sun[1]*

[1]Department of Orthopaedic Surgery, The Fourth Affiliated Hospital of Nanjing Medical University, Nanjing, China
[2]Department of Traumatic Surgery, Emergency Center, Shanghai East Hospital, Tongji University School of Medicine, Shanghai, China

Submitted: 9 May 2025; **Accepted:** 12 September 2025
Online publication: 30 December 2025

Arch Med Sci
DOI: https://doi.org/10.5114/aoms/210615

***Corresponding authors:**
Fan Sun MD
Department of Orthopaedic Surgery
The Fourth Affiliated Hospital of Nanjing Medical University
No. 298, Nanpu Road
Jiangbei New District
Nanjing, China, 210000
E-mail: sfysunfan@163.com

Guang Li, MD
Department of Traumatic Surgery
Emergency Center
Shanghai East Hospital
Tongji University School of Medicine
No. 150 Jimo Road
Pudong New Area
Shanghai, China, 200120
E-mail: guanglieast@gmail.com

Abstract

Introduction: Osteoarthritis (OA) is characterized by chronic synovial inflammation, in which synovial macrophages (SMs) play a crucial role. The contribution of JAG1 to macrophage polarization in OA remains unclear.
Material and methods: Differentially expressed genes (DEGs) were identified by analyzing the GSE64394, GSE55457, and GSE1919 datasets. An *in vitro* OA model was created. The effects on Notch signaling and macrophage polarization were assessed in IL-1β-treated fibroblast-like synoviocytes (FLS) co-cultured with SMs. *JAG1* expression was manipulated by siRNA knockdown and overexpression, and downstream effects were assessed using quantitative reverse transcription polymerase chain reaction (qRT-PCR) and Western blotting (WB).
Results: Eleven overlapping DEGs, including *JAG1*, *IL6*, *TGFB2*, *CX3CL1*, and *MMP1* were identified. Through the construction of cellular models, these genes were found to be potentially associated with inflammation, immune regulation, and extracellular matrix remodeling in OA. Additionally, the OA model was shown to induce polarization of SMs toward the M1 phenotype. *In vitro* experiments revealed that *JAG1* was significantly upregulated in OA samples. *JAG1* knockdown in the co-culture model reduced M1 markers (*NOS2*, *PTGS2*, *CD64*, *CD86*), increased M2 markers (*CD206*, *CD163*), and suppressed Notch signaling, while *JAG1* overexpression reversed these effects.
Conclusions: *JAG1* promotes the polarization of SMs toward M1 in OA by activating the Notch signaling pathway, providing preliminary evidence that the JAG1/Notch axis may serve as a potential therapeutic target for regulating inflammation and tissue remodeling in OA.

Key words: *JAG1*, Notch signaling pathway, osteoarthritis, synovial macrophages, M1 polarization, inflammation, macrophage polarization regulation.

Introduction

The degenerative joint condition known as osteoarthritis (OA) is typified by synovial inflammation, subchondral bone remodeling, and a gradual loss of articular cartilage [1]. Recent findings suggest that this cartilage loss is closely associated with inflammatory signaling; for example, miR-106a was shown to mitigate cartilage damage by targeting DR6 and modulating the NF-κB pathway in OA models [2]. OA is characterized by chronic low-grade inflammation, which promotes the pro-

duction of pro-inflammatory cytokines such as interleukin-1β (IL-1β) and tumor necrosis factor-α (TNF-α), leading to cartilage degradation and joint damage [3]. In addition, a persistent inflammatory environment promotes fibrosis of the synovium and other joint tissues, further exacerbating joint stiffness, and impairs joint function [4]. Elevated levels of IL-18 and IL-20 have also been detected in both serum and synovial fluid of OA patients, and are positively correlated with markers of cartilage turnover such as MMP-3 and YKL-40, further supporting the role of inflammation in driving cartilage breakdown [5]. In the later stages of OA, surface fibrin deposition and fibrosis are commonly observed within the synovium [6]. Fibrotic changes disrupt normal tissue structure, hinder repair processes, and exacerbate disease progression [7]. Therefore, understanding the interaction between inflammation and fibrosis is critical to developing targeted therapies for OA.

A key intercellular signaling pathway is the Notch signaling system, which regulates various cellular processes. Activation of Notch receptors occurs via engagement with ligands, such as *JAG1*, triggering intracellular signaling cascades that affect gene expression [8]. Recent studies have revealed that *JAG1* is significantly upregulated in osteoarthritic tissues, particularly in the cartilage and synovial lining. For instance, Karlsson *et al.* detected abundant expression of Notch1, *JAG1*, and *HES5* in OA-affected joints, indicating heightened Notch activity in the OA microenvironment [9]. Moreover, *JAG1* has been implicated in modulating inflammatory damage in OA; Qi *et al.* demonstrated that E3 ubiquitin ligase *ITCH* regulates JAG1 levels and alleviates chondrocyte injury under inflammatory conditions [10]. In parallel, Notch signaling has been shown to influence macrophage behavior, especially in driving M1 polarization. Activation of the Notch pathway skews macrophages toward a pro-inflammatory phenotype, exacerbating tissue inflammation and fibrosis in OA [11–13]. These findings suggest that JAG1-mediated Notch activation may contribute to macrophage-driven inflammation in OA, providing a rationale for exploring its role as a potential therapeutic target. Notch signaling is also involved in macrophage polarization in immune regulation. By regulating the equilibrium between the phenotypes of pro-inflammatory M1 and anti-inflammatory M2 macrophages, *JAG1*-mediated Notch activation can shape immune responses and tissue remodeling [14]. Jagged1 (*JAG1*) is a membrane-bound ligand of the Notch signaling pathway that binds to Notch receptors on neighboring cells to initiate signaling cascades that regulate gene expression [15]. This interaction is essential for various biological processes, including embryogenesis, tissue homeostasis, and immune responses [16]. Studies have shown that dysregulation of *JAG1* or the Notch pathway is associated with various diseases. Xiao *et al.* demonstrated that hypermethylation of the *HOXA5* gene reduces *HOXA5* expression, thereby activating *JAG1* and the Notch signaling pathway, leading to renal fibrosis [17]. Similarly, Li *et al.* found that the IGF2BP3/Notch/JAG1 pathway regulates hepatic stellate cell (HSC) ferroptosis, and *IGF2BP3* deficiency reduces *JAG1* expression, inactivates Notch signaling, and promotes HSC ferroptosis [18]. Both studies highlight the important roles of *JAG1* and Notch signaling in different diseases and propose promising therapeutic targets.

This research investigated the expression and functional function of *JAG1* in the OA inflammatory microenvironment, focusing on its effects on synovial macrophage polarization and the associated Notch signaling pathway. The upregulation of *JAG1* in OA models promotes macrophage polarization toward the pro-inflammatory M1 phenotype, which contributes to tissue remodeling and disease progression. Through activation of the Notch signaling pathway, *JAG1* modulates macrophage behavior, providing preliminary evidence for its potential role in regulating inflammation in OA. These findings may offer new insights into therapeutic strategies for managing OA and alleviating its associated inflammatory processes.

Material and methods

Downloading and processing of the datasets

GSE64394, GSE55457, and GSE1919 datasets were obtained from Gene Expression Omnibus (GEO, https://www.ncbi.nlm.nih.gov/gds/). The GSE64394 dataset contains 2 OA samples and 5 normal samples. The GSE55457 dataset contains 23 arthritis samples (10 OA, 13 rheumatoid arthritis) and 10 normal samples. The GSE1919 dataset contains 10 arthritis samples (5 OA, 5 rheumatoid arthritis) and 5 normal samples. After converting the probe IDs in the GSE64394 dataset into gene symbols, differential gene expression analysis was performed using the Limma package in R [19], which is based on linear models and empirical Bayes statistics. Genes having a fold change (FC) threshold greater than two were classified as up-regulated differentially expressed genes (DEGs), while those with an FC < 0.5 were considered down-regulated DEGs. A p-value < 0.05 was used as the significance threshold.

Identification and expression analysis of genes in OA

Protein–protein interactions (PPI) of DEGs in the GSE64394 dataset were performed by the Search

Tool for the Retrieval of Interacting Genes/Proteins (STRING, https://string-db.org/), providing insights into their functional associations [20]. Cytoscape software (version 3.7.1) was used for analyzing the PPI network, created using the Degree of Maximum Neighborhood Component (DMNC) and Molecular Complex Detection (MCODE) algorithms [21]. A bioinformatics program (https://bioinformatics.psb.ugent.be/webtools/Venn/) then found DEGs from the DMNC and MCODE networks that overlapped. To evaluate the expression levels of these overlapping DEGs, data processing and visualization were carried out in R. The expression profiles of the selected genes in the case and normal groups of the GSE64394, GSE1919, and GSE55457 datasets were examined using box plot analysis.

Cell lines and culture

We acquired human synovial macrophages (SMs) and fibroblast-like synoviocytes (FLS) from the American Type Culture Collection (ATCC). Additionally, 10% fetal bovine serum (FBS) and 1% penicillin-streptomycin (100 U/ml penicillin and 100 µg/ml streptomycin) were added to Dulbecco's Modified Eagle Medium (DMEM) for their maintenance. Cell cultures were kept in a humidified environment with 5% CO_2, at 37°C.

Cell treatment and co-culture

To mimic the inflammatory microenvironment in OA, FLSs were treated with 10 ng/ml of recombinant mouse IL-1β protein (C042, Novoprotein, Shanghai), as previously described [22], which was used as a model for OA. FLS cells not treated with IL-1β were used as the control group. After 24 h of IL-1β stimulation, the medium was thoroughly removed to eliminate residual IL-1β, and FLSs were washed with PBS before proceeding to co-culture. This approach was adapted from a previously established method for generating persistently activated stromal cells [23]. For co-culture experiments, the top chamber of a Transwell system (0.4-µm pore size, Corning, USA) was used to seed SMs at a density of 2×10^5 cells/well, while FLSs were plated in the lower chamber at the same density. The co-cultures were maintained in the same medium over 48 h with 10 ng/ml of recombinant human IL-1β. After that, cells were collected for further examination.

Cell transfection

To achieve transient overexpression and knockdown expression of *JAG1*, we placed cells in 24-well plates containing 2×10^5 cells per well. We used a pcDNA3.1-based plasmid encoding full-length human *JAG1* for overexpression, as well as three siRNAs targeting *JAG1* mRNA (si-*JAG1*-1, si-*JAG1*-2, si-*JAG1*-3). The siRNA sequences were as follows: si-*JAG1*-1: CGCGUGACCUGUGAUGACUACUACU (Sense Sequence), AGUAGUAGUCAUCACAGGUCACGCG (Antisense Sequence); si-*JAG1*-2: CAGUCCUAAGCAUGGGGUCUUUGCAAA (Sense Sequence), UUUGCAAGACCCAUGCUUUAGGACUG (Antisense Sequence); si-*JAG1*-3: AACGUGCCAGUUAGAUGCAAAUGAA (Sense Sequence), UUCAUUUGCAUCUAACUGGCACGUUU (Antisense Sequence); si-NC: CAGUCAACGUAGGUGUCGUCCUAAA (Sense Sequence), UUUUAGGACGACACCUACGUUGACUG (Antisense Sequence). During transfection, we used siRNA at a final concentration of 50 nM and plasmid DNA at a concentration of 2 µg/ml. We used Lipofectamine 3000 (Invitrogen, China) reagent, adding 1 µl per well and following the manufacturer's instructions. Forty-eight hours after transfection, we analyzed the expression level of *JAG1* by qRT-PCR and WB to assess the transfection efficiency.

Quantitative reverse transcription polymerase chain reaction (qRT-PCR)

Following the manufacturer's instructions, TRIzol reagent (Tiangen, Beijing, China) was used to extract total RNA from cells. RNA concentration and purity were evaluated with a Thermo Fisher Scientific NanoDrop spectrophotometer. A Takara Reverse Transcription Kit (Dalian, China) was applied to create cDNA from 1 µg of total RNA according to the provided protocol. SYBR Green Master Mix (Applied Biosystems) was applied for qRT-PCR via an ABI 7500 Real-Time PCR System (Applied Biosystems). *GAPDH* was used as the internal reference gene due to its stable expression across experimental conditions. The $2^{-\Delta\Delta CT}$ technique was applied to determine the relative expression levels of the target genes. Table I lists the primer sequences employed in qRT-PCR.

Western blot (WB) assay

The experiment was conducted following the usual WB experimental protocols [24]. Cells were lysed, and total protein concentrations were determined using a BCA Protein Assay Kit (Beyotime, Shanghai, China). Equal amounts of protein were separated by SDS-PAGE, transferred to PVDF membranes (Beyotime, Shanghai, China), and blocked in 5% skim milk. Membranes were incubated overnight at 4°C with primary antibodies including NOS2 (ab15323, 1 : 10000), PTGS2 (ab188184, 1 : 1000), CD64 (ab140779, 1 : 4000), CD86 (ab239075, 1 : 1000), CD206 (ab64693, 1 : 5000), CD163 (ab182422, 1 : 1000), JAG1 (ab109536, 1 : 1000), Hes1 (ab71559, 1 : 200), Hes5 (ab194111, 1 : 1000), Hey1 (ab154077, 1 :

Table I. Primer sequences for qRT-PCR

Target	Direction	Sequence (5′-3′)
IL-8	Forward	CTCCAAACCTTTCCACCCCA
IL-8	Reverse	TTCTCAGCCCTCTTCAAAAACT
CTGF	Forward	TTAGCGTGCTCACTGACCTG
CTGF	Reverse	GCCACAAGCTGTCCAGTCTA
CXCL1	Forward	TTCACAGTGTGTGGTCAACAT
CXCL1	Reverse	AGCCCCTTTGTTCTAAGCCA
ACTA2	Forward	GTTCCGCTCCTCTCTCCAAC
ACTA2	Reverse	ACGCTGGAGGACTTGCTTTT
CYR61	Forward	AATACCGGCCCAAGTACTGC
CYR61	Reverse	GCCTGTAGAAGGGAAACGCT
CEMIP	Forward	ACCCATCACTCGGTCTCTGA
CEMIP	Reverse	CAGCATGGCCTTGAAGAGGA
NOS2	Forward	GCCATAGAGATGGCCTGTCC
NOS2	Reverse	GGGGACTCATTCTGCTGCTT
PTGS2	Forward	GGCCATGGGGTGGACTTAAA
PTGS2	Reverse	ACCGTAGATGCTCAGGGACT
CD64	Forward	CTGCTCCTTTGGGTTCCAGT
CD64	Reverse	GATTCTGTAGCTGGGGGTCG
CD86	Forward	TGCTGTAACAGGGACTAGCAC
CD86	Reverse	AAGTTAGCAGAGAGCAGGAAGG
CD206	Forward	ACCTGCGACAGTAAACGAGG
CD206	Reverse	TGTCTCCGCTTCATGCCATT
CD163	Forward	GAAGACAGAGACAGCGGCTT
CD163	Reverse	GGTATCTTAAAGGCTCACTGGGT
JAG1	Forward	TCACGGGAAGTGCAAGAGTC
JAG1	Reverse	GTTTCACAGTAGGCCCCCTC
Hes1	Forward	TTTCCTCATTCCCAACGGGG
Hes1	Reverse	GGTGGGTTGGGGAGTTTAGG
Hes5	Forward	AGAGAAAAACCGACTGCGGA
Hes5	Reverse	GACGAAGGCTTTGCTGTGC
Hey1	Forward	AGTGCGGACGAGAATGGAAA
Hey1	Reverse	TGCTCCATTACCTGCTTCTCAA
Hey2	Forward	ACAATTACTCGGGGCAAAGT
Hey2	Reverse	GCAGTTGGCACAAGTCTTCTC
GAPDH	Forward	AATGGGCAGCCGTTAGGAAA
GAPDH	Reverse	GCGCCCAATACGACCAAATC

Primer sequences for target genes, including forward and reverse sequences, are provided for qRT-PCR analysis. GAPDH was used as the internal reference gene for normalization.

500), and Hey2 (ab167280, 1 : 2500) (Abcam, China). GAPDH (ab181602, Abcam, China, 1: 10000) served as an internal reference. Protein bands were visualized using an enhanced chemiluminescence (ECL) kit (Tiangen, Beijing, China) and captured using a ChemiDoc imaging system (Bio-Rad, Shanghai, China). Band intensities were quantified using ImageJ software (version 1.80) and normalized to GAPDH levels. Exposure times were adjusted to ensure detection within the linear dynamic range.

Enzyme-linked immunosorbent assay (ELISA)

According to the manufacturers' instructions, commercially available ELISA kits (all purchased from Abcam, Cambridge, UK) were used to measure the concentrations of M1 markers (NOS2, PTGS2, CD64, CD86, IL-6, TNF-α) and M2 markers (CD206, CD163, IL-10, Arg1) in cell culture supernatants or cell lysates. Briefly, samples and standards were added to 96-well plates pre-coated with specific capture antibodies and incubated at room temperature for 2 h. After washing, biotinylated detection antibodies were added and incubated for 1 h, followed by streptavidin-HRP conjugate for 30 min. Plates were washed again, and TMB substrate solution was added for color development. The reaction was stopped with stop solution, and absorbance was measured at 450 nm using a microplate reader (Bio-Rad, USA).

Statistical analysis

Statistical analyses were performed using R software. All experiments were independently repeated at least three times using separate cell cultures to ensure reproducibility. Data are presented as mean ± standard deviation (SD). One-way analysis of variance (ANOVA) was used to assess statistical differences among groups, followed by Tukey's post-hoc test. A p-value < 0.05 was considered statistically significant.

Results

Identification and expression analysis of DEGs in OA

251 upregulated and 235 downregulated DEGs were recognized from the GSE64394 dataset by the R package (Figure 1 A). PPI network analysis was performed using two algorithms, DMNC and MCODE. The DMNC algorithm identified the top 20 genes, while MCODE identified the top 25 genes (Figures 1 B, C). Further analysis through a bioinformatics platform revealed 11 overlapping genes between the two algorithms (Figure 1 D). Expression analysis demonstrated that *CCR1*, *CD276*, *CX3CL1*, *JAG1*, *MMP1*, *OCLN*, *TGFA*, *TGFB2*, and *TGFB3* were markedly increased in case samples of the GSE64394 dataset, whereas *PDCD1LG2* and *TSLP* were significantly upregulated in normal samples (Figure 1 E). Validation in the GSE1919 dataset confirmed significant upregulation of *CCR1*, *CX3CL1*, *JAG1*, *MMP1*, *OCLN*, *TGFA*, *TGFB2*, and *TGFB3* in case samples (Figure 1 F).

In contrast, analysis of the GSE55457 dataset revealed that *CCR1*, *JAG1*, *OCLN*, *TGFA*, *TGFB2*, and *TGFB3* were significantly downregulated in case samples, whereas *CX3CL1*, *MMP1*, and *PDCD1LG2* were significantly upregulated (Figure 1 G).

High expression of inflammatory response factors in OA models

IL8 and *CXCL1* are critical mediators of inflammatory responses in OA, contributing to immune cell recruitment as well as the activation of matrix-degrading enzymes [25]. *CTGF* and *CYR61* promote angiogenesis and extracellular matrix remodeling, respectively, aiding cartilage repair and destruction [26]. Furthermore, *ACTA2* and *CEMIP* are strongly linked to OA-related synovial inflammation and gradual loss of joint function [27]. qRT-PCR analysis revealed a substantial increase of *IL8*, *CTGF*, *CXCL1*, *ACTA2*, *CYR61*, and *CEMIP* in the OA model compared with the control group (FLSs without IL-1β stimulation). These findings

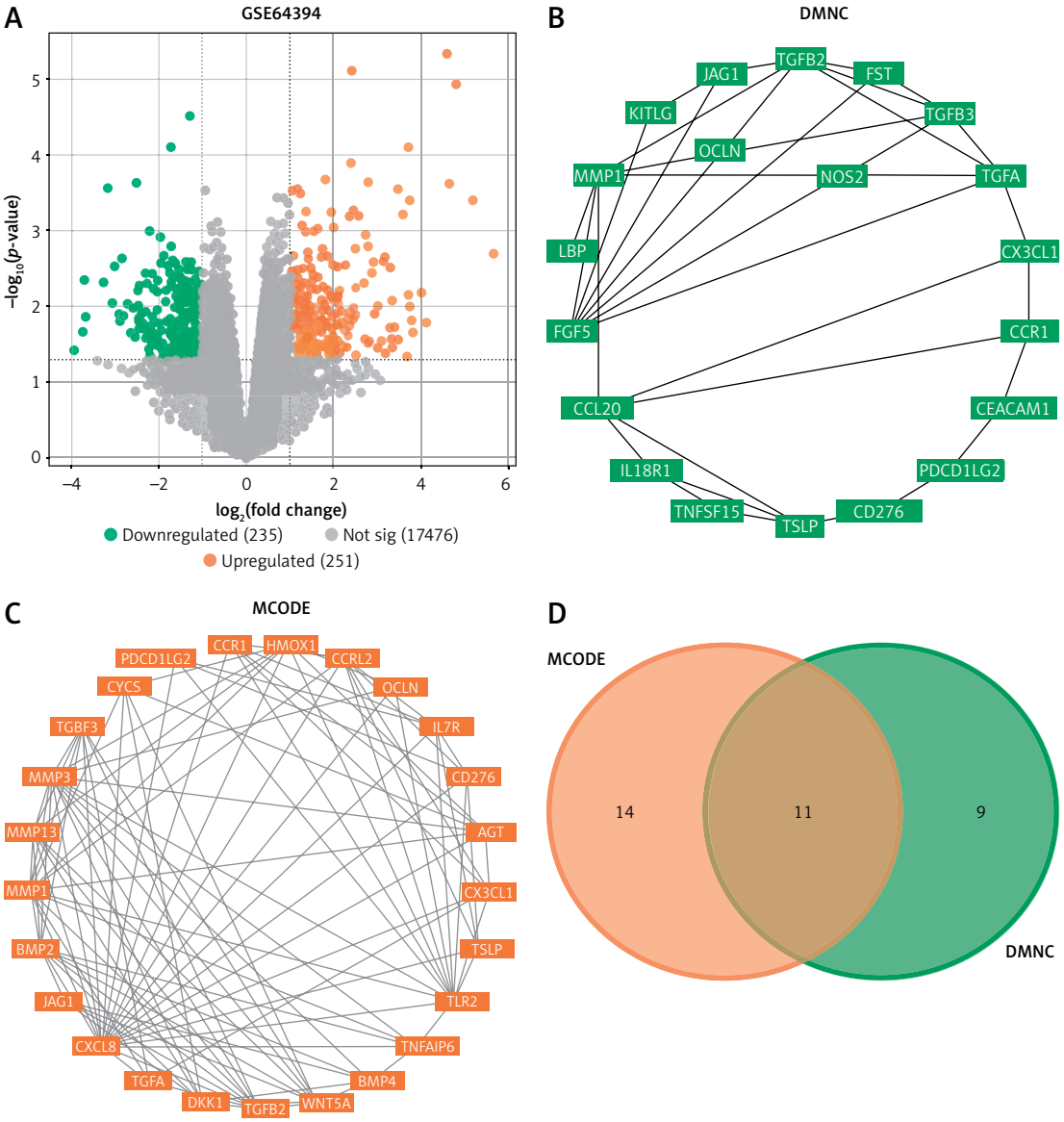

Figure 1. Identification and expression analysis of differentially expressed genes (DEGs) in osteoarthritis (OA). **A** – Volcano plot of 251 upregulated and 235 downregulated DEGs identified from the GSE64394 dataset using the R package. Orange indicates up-DEGs, and green indicates down-DEGs. **B** – Protein–protein interaction (PPI) network of DEGs generated using the Degree of Maximum Neighborhood Component (DMNC) algorithm, displaying the top 20 DEGs based on their interaction strength. Nodes represent genes, and edges represent PPI. **C** – PPI network of DEGs generated using the Molecular Complex Detection (MCODE) algorithm, showing the top 25 DEGs. The network was visualized to highlight the most interconnected genes. **D** – Venn diagram illustrating the 11 overlapping DEGs identified between the DMNC and MCODE algorithms, representing genes common to both networks. *$P < 0.05$. **$P < 0.01$

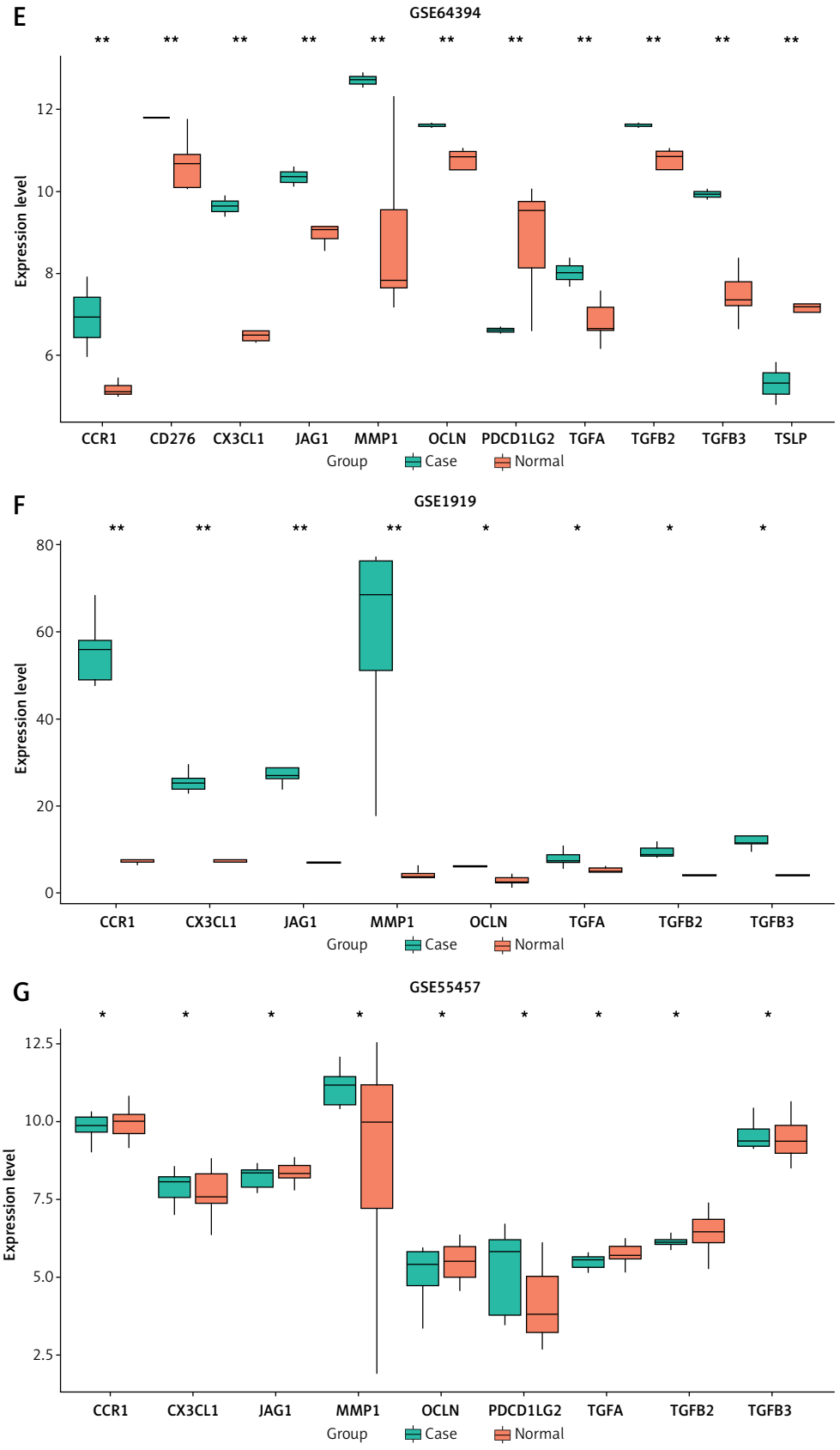

Figure 1. Cont. **E**–**G** – Box plots showing the expression levels of overlapping DEGs in the case and normal samples in GSE64394 (**E**), GSE1919 (**F**), and GSE55457 (**G**) datasets. *$P < 0.05$. **$P < 0.01$

highlight that these genes are closely linked to the inflammatory and pathological processes of OA (Figures 2 A–F).

OA model induces SMs to polarize toward M1

NOS2, *PTGS2*, *CD64*, and *CD86* were used as M1 markers, while *CD206* and *CD163* were used as M2 markers [28]. The expression levels of these markers in SMs or SMs co-cultured with the OA model were examined by WB and qRT-PCR. It was found that exposure to the OA model promoted a pro-inflammatory M1 macrophage phenotype, characterized by elevated inflammatory marker expression, and suppressed anti-inflammatory M2 markers (Figures 3 A–F). These results suggest that the OA environment reshapes macrophage

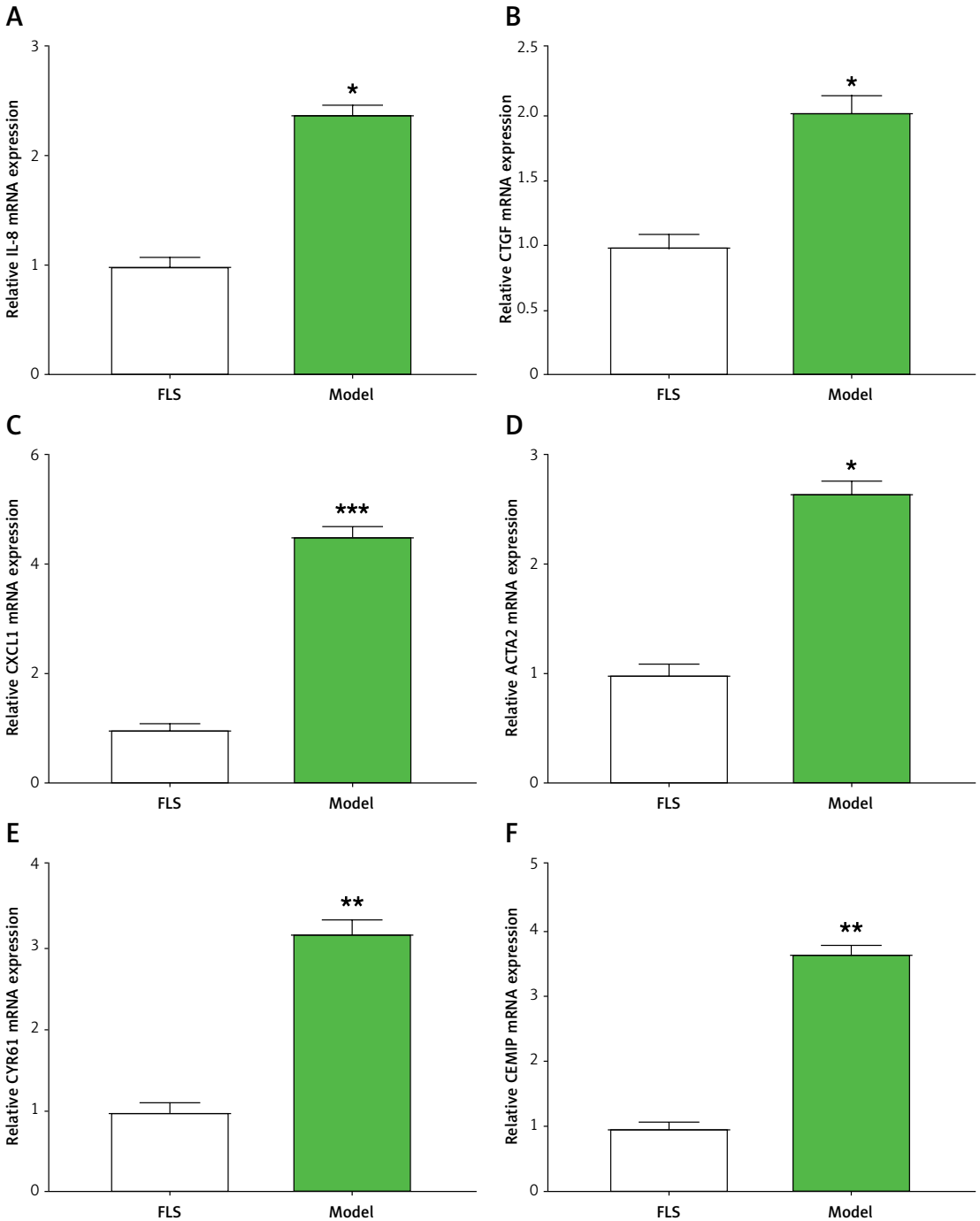

Figure 2. High expression of inflammatory response factors in OA models. **A–F** – Quantitative reverse transcription polymerase chain reaction (qRT-PCR) detection of mRNA expression of *IL-8*, *CTGF*, *CXCL1*, *ACTA2*, *CYR61*, and *CEMIP* in fibroblast-like synoviocytes (FLS) cells and OA models. *IL-8*, *CTGF*, *CXCL1*, *ACTA2*, *CYR61*, and *CEMIP* are OA-related genes. **P* < 0.05. ***P* < 0.01. ****P* < 0.001

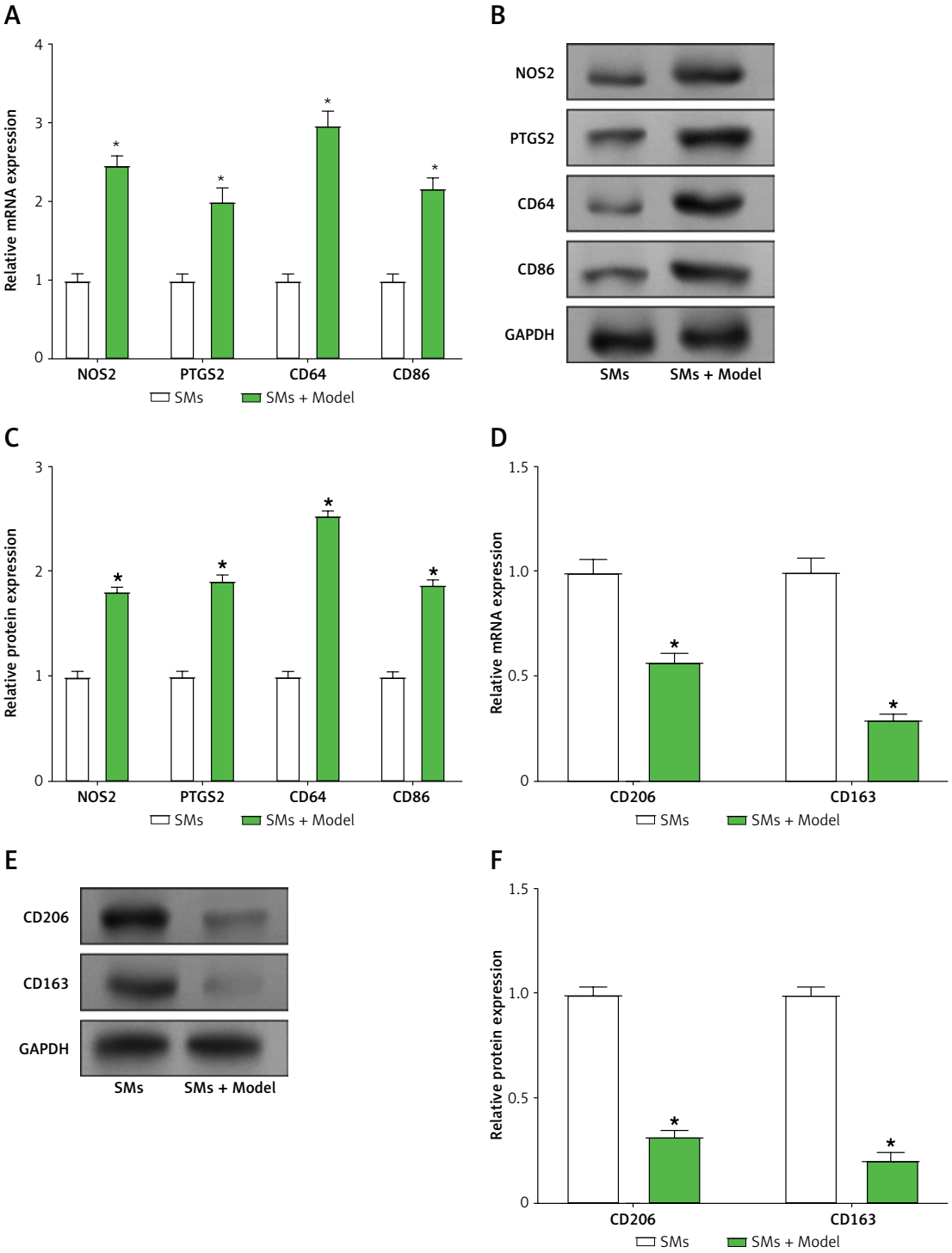

Figure 3. Changes in M1 and M2 polarization markers in macrophages cultured alone (SMs) co-cultured with FLS from the OA model. **A** – Relative mRNA expression levels of M1 polarization markers (*NOS2*, *PTGS2*, *CD64*, and *CD86*) in SMs and SMs + OA models (macrophages co-cultured with OA model). **B** – Representative protein blot images of M1 polarization markers (NOS2, PTGS2, CD64, and CD86) in SMs and SMs + OA models. **C** – Quantification of protein expression levels of M1 markers based on Western blot analysis. **D** – Relative mRNA expression levels of M2 polarization markers (*CD206* and *CD163*) in SMs and SMs + Model. **E** – Representative Western blot images of M2 markers (CD206 and CD163) in SMs and SMs + Model. **F** – Quantification of protein expression levels of M2 markers based on Western blot analysis. *$P < 0.05$

polarization, which may help sustain synovial inflammation and influence OA progression.

JAG1 is highly expressed in OA models

qRT-PCR and WB analyses revealed that the expression of JAG1 was considerably upregulated in FLSs from the OA model compared to the control group (untreated FLSs) (Figures 4 A–C). To investigate the regulatory effects of *JAG1*, three *JAG1*-specific siRNAs (si-*JAG1*-1, si-*JAG1*-2, and si-*JAG1*-3) were transfected into the OA model. All three siRNAs efficiently lowered *JAG1* mRNA and protein levels, with si-*JAG1*-2 having the great-

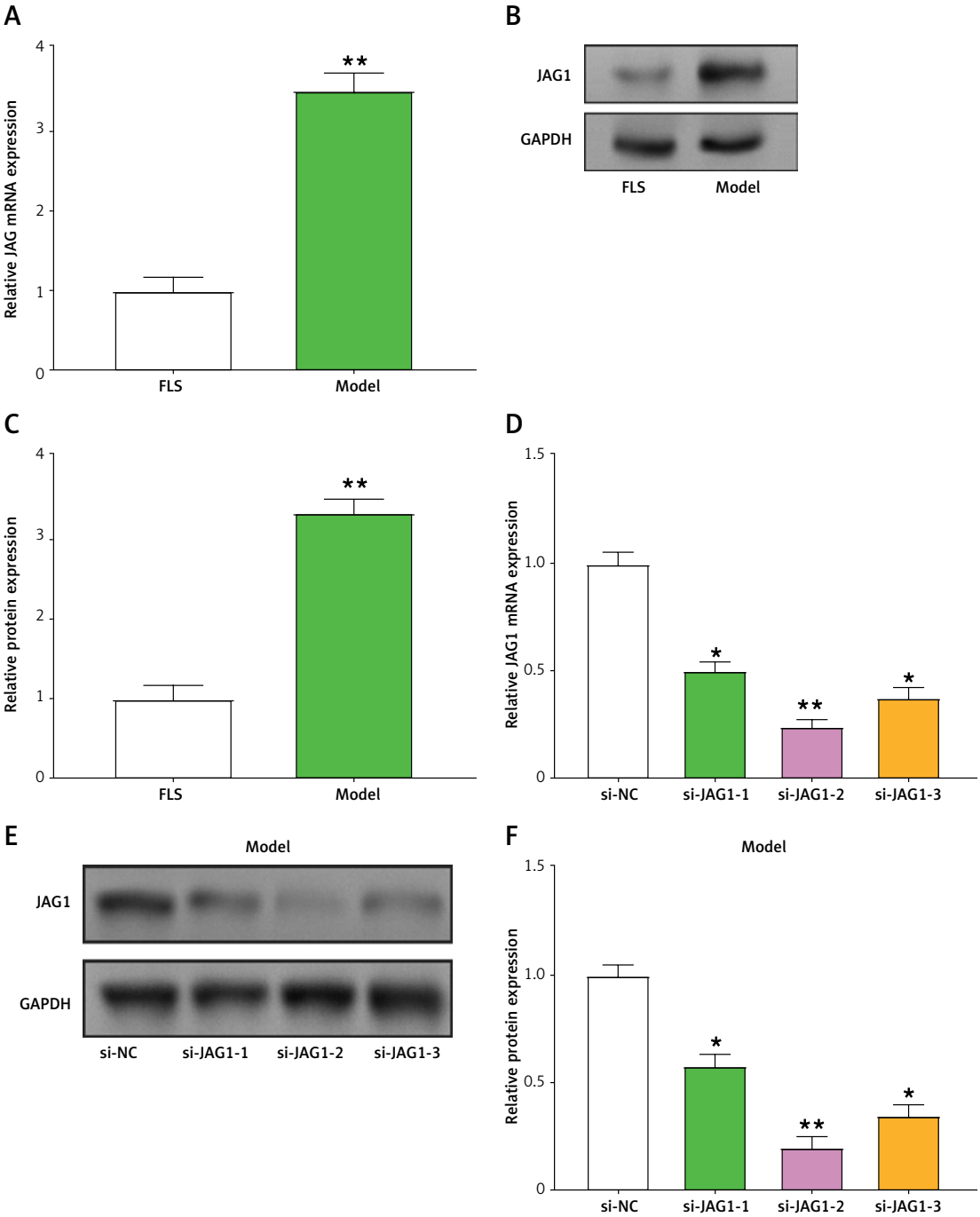

Figure 4. *JAG1* is highly expressed in OA models. **A** – Relative mRNA expression of *JAG1* in the OA model and control group. **B** – Representative protein blot images of JAG1 protein expression in OA models and controls. **C** – Quantification of JAG1 protein levels based on Western blot analysis. **D** – Relative mRNA expression of *JAG1* in OA model transfected with three *JAG1*-specific siRNAs (si-*JAG1*-1, si-*JAG1*-2, si-*JAG1*-3) and one negative control siRNA (small interfering RNA negative control – si-NC). **E** – Representative protein blot images of JAG1 protein expression in OA models transfected with siRNA. **F** – Quantification of JAG1 protein levels based on Western blot analysis. **P* < 0.05. ***P* < 0.01

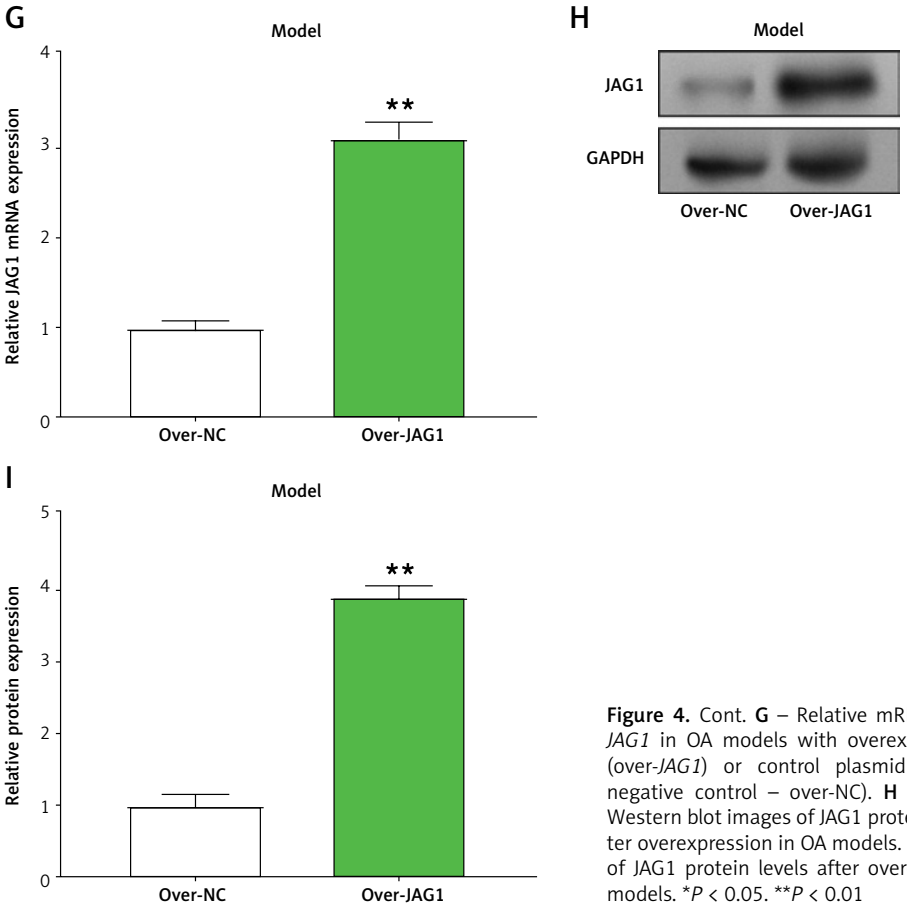

Figure 4. Cont. **G** – Relative mRNA expression of *JAG1* in OA models with overexpression plasmid (over-*JAG1*) or control plasmid (overexpression negative control – over-NC). **H** – Representative Western blot images of JAG1 protein expression after overexpression in OA models. **I** – Quantification of JAG1 protein levels after overexpression in OA models. **P* < 0.05. ***P* < 0.01

est knockdown effectiveness (Figures 4 D–F). In contrast, overexpression of *JAG1* in the OA model resulted in a significant rise in *JAG1* mRNA and protein levels compared to the control group (over-NC) (Figures 4 G–I).

JAG1 promotes polarization of SMs toward M1 in the OA model

SMs were co-cultured with the OA model and transfected with si-*JAG1*-2 to investigate the impact of *JAG1* on macrophage polarization. A qRT-PCR investigation indicated notable alterations of M1 and M2 markers. Compared to SMs cultured alone, co-culture with the OA model led to substantial upregulation of M1 markers (*NOS2*, *PTGS2*, *CD64*, and *CD86*), and marked downregulation of M2 markers, including *CD206* and CD163. Importantly, these changes were reversed upon si-*JAG1*-2 transfection, indicating that *JAG1* plays a pivotal role in modulating macrophage polarization toward the M1 phenotype (Figures 5 A–F). In addition, the WB results corroborated the qRT-PCR findings, showing consistent patterns of protein expression. M1 markers were downregulated, whereas M2 markers were upregulated following si-*JAG1*-2 transfection, which further confirmed that *JAG1* promotes the polarization of SMs toward M1 in the OA model (Supplementary Figures S1 A–H). These outcomes highlight the crucial role of *JAG1* in regulating synovial macrophage polarization in the context of OA.

JAG1 promotes polarization of SMs to M1 by activating the Notch signaling pathway in OA models

qRT-PCR and WB analysis demonstrated that *JAG1* knockdown dramatically reduced the expression of downstream genes associated with the Notch signaling pathway, including *Hes1*, *Hes5*, *Hey1*, and *Hey2* (Figures 6 A–C). However, overexpression of *JAG1* reversed these changes (Figures 7 A–D, Supplementary Figures S2 A–E). In addition, the degrees of manifestation of M1 and M2 polarization markers were evaluated after *JAG1* knockdown or combined with *JAG1* overexpression. Compared to SMs alone, co-culture with the OA model led to significant upregulation of M1 markers and marked downregulation of M2 markers. Induction of si-*JAG1*-2 attenuated these changes, while subsequent *JAG1* overexpression reversed the attenuation (Figures 7 E–J, Supplementary Figures S2 F–M, S3). These results suggest that *JAG1* modulates Notch signaling and influences macrophage polarization in the OA microenvironment,

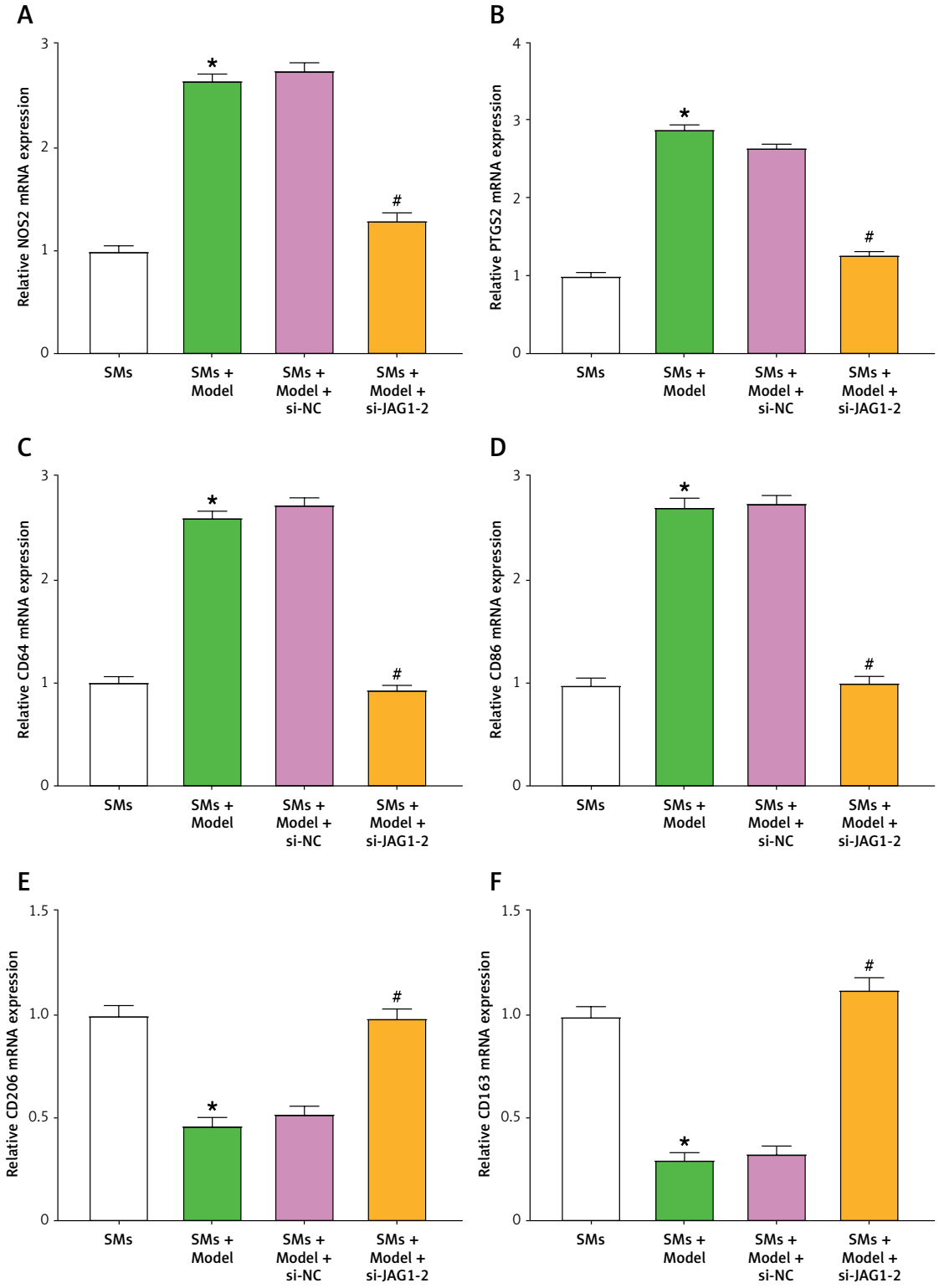

Figure 5. *JAG1* knockdown reduces M1 polarization and enhances M2 polarization in SMs co-cultured with the OA model. **A**–**D** – Relative mRNA expression levels of M1 polarization markers (*NOS2*, *PTGS2*, *CD64*, and *CD86*) in SMs, SMs + Model, SMs + Model + si-NC, and SMs + Model + si-*JAG1*-2. **E**, **F** – Relative mRNA expression levels of M2 polarization markers (*CD206* and *CD163*) across the same experimental groups. **P* < 0.05 vs. SMs. #*P* < 0.05 vs. SMs + Model

SMs – macrophages cultured alone; SMs + Model – macrophages co-cultured with OA model; SMs + Model + si-NC – macrophages co-cultured with OA model transfected with si-NC; SMs + Model + si-JAG1-2 – macrophages co-cultured with OA model transfected with si-JAG1-2.

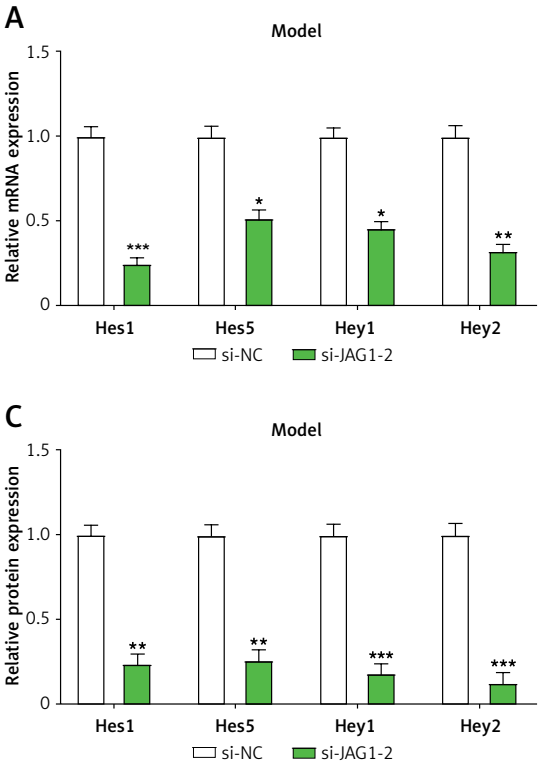

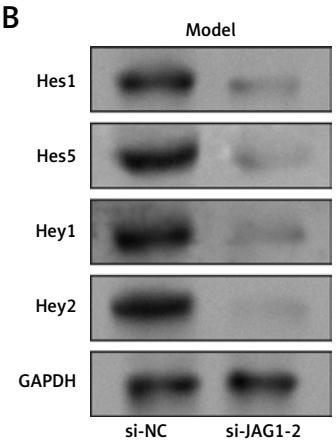

Figure 6. *JAG1* activates the Notch signaling pathway in the OA model. **A** – Relative mRNA expression levels of Notch signaling downstream genes (*Hes1*, *Hes5*, *Hey1*, and *Hey2*) in OA model transfected with negative control siRNA (si-NC) or *JAG1*-specific siRNA (si-*JAG1*-2), as measured by qRT-PCR. **B** – Representative Western blot images showing the protein expression levels of Hes1, Hes5, Hey1, and Hey2 in the same experimental groups. **C** – Quantification of protein expression levels based on Western blot analysis. *$P < 0.05$. **$P < 0.01$. ***$P < 0.001$

highlighting its potential role in regulating inflammation and tissue remodeling in OA.

Discussion

Degradation of cartilage and inflammation are hallmarks of OA, a chronic degenerative joint condition. Inflammatory factors play a central role in the development of OA [29]. Interleukin-8 (IL-8) promotes neutrophil recruitment and inflammation, while connective tissue growth factor (CTGF) enhances fibrosis and joint stiffness [30]. Chemokine (C-X-C motif) ligand 1 (CXCL1) contributes to immune cell migration and inflammation. Actin alpha 2, smooth muscle (ACTA2) is involved in fibrosis and tissue remodeling [31]. Cysteine rich angiogenic inducer 61 (CYR61) regulates cell adhesion and proliferation, and cell migration inducing hyaluronidase 1 (CEMIP) is linked to cartilage degradation [32]. These inflammatory mediators collectively exacerbate tissue damage, driving

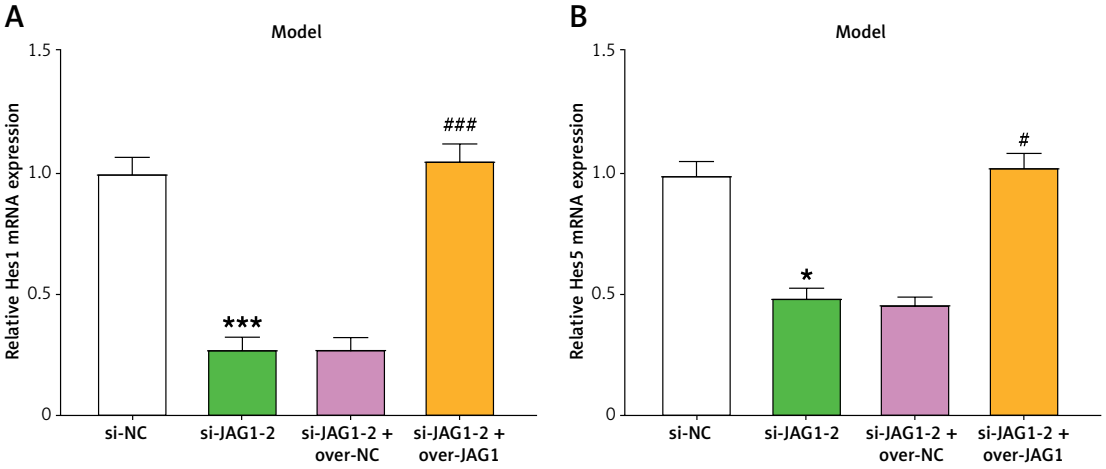

Figure 7. *JAG1* promotes the polarization of SMs to M1 by activating the Notch signaling pathway in the OA model. **A, B** – The relative mRNA expression of *Hes1*, *Hes5*, *Hey1*, and *Hey2* in the OA model after transfection with si-*JAG1*-2 and si-*JAG1*-2+over-*JAG1* was detected by qRT-PCR. *$P < 0.05$, **$P < 0.01$, ***$P < 0.001$ vs. si-NC. $^{\#}P < 0.05$, $^{\#\#}P < 0.01$, $^{\#\#\#}P < 0.001$ vs. si-*JAG1*-2 + over-NC

over-NC – overexpression negative control; SMs – macrophages cultured alone; SMs + Model – macrophages co-cultured with OA model; SMs + Model + si-JAG1-2 + over-NC – macrophages co-cultured with OA model transfected with si-JAG1-2 and over-NC; SMs + Model + si-JAG1-2 + over-JAG1 – macrophages were co-cultured with OA models transfected with si-JAG1-2 and over-JAG1.

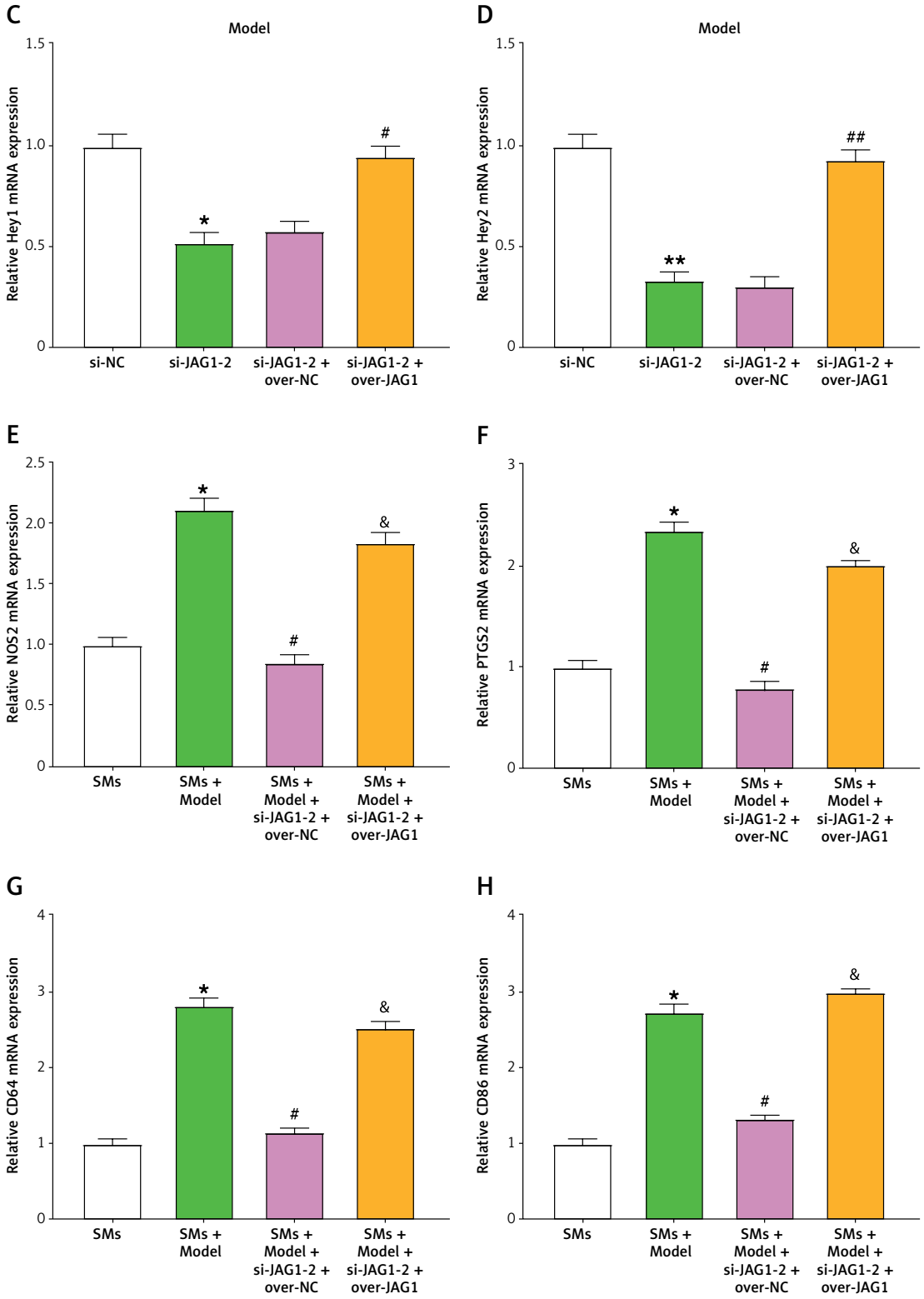

Figure 7. Cont. **C, D** – The relative mRNA expression of *Hes1*, *Hes5*, *Hey1*, and *Hey2* in the OA model after transfection with si-*JAG1*-2 and si-*JAG1*-2+over-*JAG1* was detected by qRT-PCR. $^{*}P < 0.05$, $^{**}P < 0.01$, $^{***}P < 0.001$ vs. si-NC. $^{\#}P < 0.05$, $^{\#\#}P < 0.01$, $^{\#\#\#}P < 0.001$ vs. si-*JAG1*-2 + over-NC. **E–H** – Relative mRNA expression of M1 polarization markers and M2 polarization markers in SMs, SMs + Model, SMs + Model + si-*JAG1*-2 + over-NC, and SMs + Model + si-*JAG1*-2 + over-*JAG1* was detected by qRT-PCR. $^{*}P < 0.05$ vs. SMs. $^{\#}P < 0.05$ vs. SMs + Model. $^{\&}P < 0.001$ vs. SMs + Model + si-*JAG1*-2 + over-NC

over-NC – overexpression negative control; SMs – macrophages cultured alone; SMs + Model – macrophages co-cultured with OA model; SMs + Model + si-JAG1-2 + over-NC – macrophages co-cultured with OA model transfected with si-JAG1-2 and over-NC; SMs + Model + si-JAG1-2 + over-JAG1 – macrophages were co-cultured with OA models transfected with si-JAG1-2 and over-JAG1.

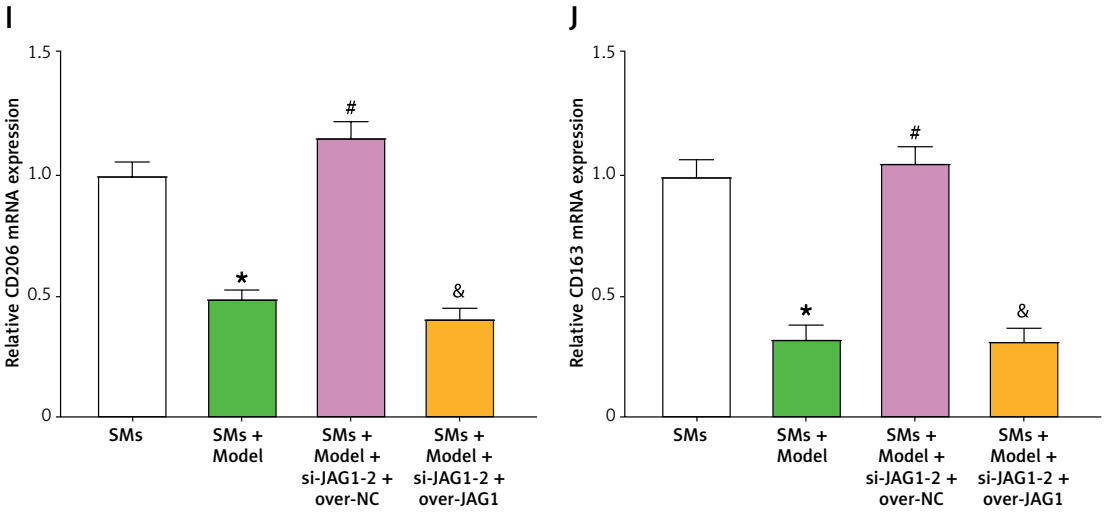

Figure 7. Cont. **I–J** – Relative mRNA expression of M1 polarization markers and M2 polarization markers in SMs, SMs + Model, SMs + Model + si-*JAG1*-2 + over-NC, and SMs + Model + si-*JAG1*-2 + over-*JAG1* was detected by qRT-PCR. **P* < 0.05 vs. SMs. #*P* < 0.05 vs. SMs + Model. &*P* < 0.001 vs. SMs + Model + si-*JAG1*-2 + over-NC

over-NC – overexpression negative control; SMs – macrophages cultured alone; SMs + Model – macrophages co-cultured with OA model; SMs + Model + si-JAG1-2 + over-NC – macrophages co-cultured with OA model transfected with si-JAG1-2 and over-NC; SMs + Model + si-JAG1-2 + over-JAG1 – macrophages were co-cultured with OA models transfected with si-JAG1-2 and over-JAG1.

OA progression. Stone *et al.* demonstrated that pro-inflammatory stimulation of meniscus cells in OA enhances the production of matrix metalloproteinases and catabolic factors, including IL-8, CTGF, CXCL1, ACTA2, CYR61, and CEMIP, contributing to joint tissue destruction and OA progression [33]. Deroyer *et al.* further revealed that *CEMIP* regulates inflammation, hyperplasia, and fibrosis in the OA synovial membrane by promoting production of inflammatory cytokines, such as IL-8 and CXCL1, and driving the epithelial-to-mesenchymal transition (EMT) pathway [34]. This leads to elevated levels of fibrotic markers such as *ACTA2* and *CTGF*, as well as synovial hyperplasia. Additionally, Maldonado *et al.* highlighted that inflammation-induced ECM remodeling in cartilage disrupts chondrocyte function, inhibits tissue repair, and exacerbates OA progression [35]. Key inflammatory factors, including IL-8 and CTGF, drive ECM alterations and cellular dysfunction. Similarly, in our study, the expression levels of inflammatory factors (*IL8*, *CXCL1*, *CYR61*, etc.) were significantly upregulated in the OA model, which emphasizes their crucial functions in the etiology of OA and the therapeutic potential of targeting inflammatory factors.

SMs are key immune cells in the joint synovium, contributing to inflammation and tissue repair [36]. Pro-inflammatory M1 or anti-inflammatory M2 phenotypes are the results of these cells' polarization. M1 macrophages, marked by *NOS2*, *PTGS2*, *CD64*, and *CD86* expression, secrete cytokines such as IL-1β and TNF-α, driving inflammation and tissue damage [37]. Conversely, M2 macrophages, characterized by *CD206* and *CD163* expression, release anti-inflammatory mediators such as IL-10, facilitating tissue repair [38]. Several studies have highlighted key mechanisms by which macrophage polarization influences OA progression. Wang *et al.* found that Nrf2 activation inhibits M1 polarization while promoting M2 polarization, reducing inflammation and aiding cartilage protection, thus underscoring its therapeutic potential [39]. Zhang *et al.* reported that M1-polarized SMs, through mTORC1 activation, enhance R-spondin-2 secretion, activating β-catenin signaling in chondrocytes and exacerbating OA [11]. Additionally, Fang *et al.* found that *TREM2* promotes M1 to M2 macrophage polarization, with *TREM2* deficiency worsening joint inflammation via NF-κB/CXCL3 signaling, while recombinant *TREM2* mitigates these effects by promoting M2 polarization and improving joint pathology [40]. Our research revealed that the OA model induces M1 polarization in SMs, as evidenced by the significant upregulation of M1 markers (*NOS2*, *PTGS2*, *CD64*, and *CD86*) and downregulation of M2 markers (*CD206* and *CD163*), as determined through qRT-PCR and Western blot analysis. This shift toward M1 polarization may contribute to the pro-inflammatory state in the OA synovium. Modulating macrophage polarization may thus represent a potential approach to attenuate synovial inflammation associated with OA.

Through bioinformatics analysis of the GSE64394 dataset, we obtained the hub gene *JAG1*, which was significantly upregulated in the case groups of the GSE64394, GSE1919, and GSE55457 datasets. In addition, *in vitro* cell experiments also proved that it was significant-

ly overexpressed in OA models. JAG1 encodes Jagged1, a transmembrane protein and ligand for the Notch signaling pathway, which is essential to cell differentiation, proliferation, and immune responses [41]. *ITCH* overexpression promotes chondrocyte proliferation, reduces inflammation, and prevents extracellular matrix degradation by inhibiting Notch1 activation, suggesting a novel therapeutic approach for OA. Notch signaling is activated when JAG1 binds to the Notch receptor, triggering a cascade of intracellular events that regulate gene expression. This interaction is essential for cell fate determination, immune cell differentiation, and tissue regeneration. Dysregulation of the JAG1-Notch pathway, including overexpression of *JAG1*, is linked to various diseases, including OA, where it influences macrophage polarization and inflammatory responses. In our study, *JAG1* promoted M1 polarization of SMs. Co-culture with the OA model upregulated M1 markers and downregulated M2 markers, which was reversed by si-*JAG1*-2 transfection. Western blot results confirmed these findings, supporting the role of *JAG1* in promoting M1 polarization. These results suggest that targeting *JAG1* may help modulate synovial inflammation by shifting macrophage phenotypes, which could be beneficial in the context of OA. Notably, the function of Jagged1 in inflammation is disease-specific. One study showed that Jagged1, a downstream target of RBP-J, inhibits TNF-induced osteoclastogenesis through a negative feedback mechanism without affecting the overall expression of inflammatory factors, suggesting a protective role in rheumatoid arthritis (RA)-associated bone destruction [42]. In another study, *JAG1* was found to be enriched in synovial macrophages from RA patients and was co-regulated by TNF and TLR signaling [43]. These studies revealed that *JAG1* may have anti-breaking and anti-inflammatory properties in RA. However, unlike the above studies, our results show that *JAG1* promotes M1 polarization and exacerbates inflammation in OA, suggesting that its function may be influenced by differences in disease type and microenvironment. Thus, our study provides additional evidence for a novel pro-inflammatory mechanism of *JAG1* in OA and provides a theoretical basis for targeting *JAG1* to intervene in OA inflammation.

Research suggests that OA activates Notch signaling. Lin NY's study showed that blocking Notch1 can increase Hedgehog signaling through a *Hes1*-dependent pathway, aggravate OA, and lead to increased cartilage degradation, osteophyte proliferation, and chondrocyte hypertrophy [44]. Research by Karlsson *et al.* showed that the levels of Notch1, Jagged1 and Hes5 are increased in osteoarthritic cartilage, and Notch signaling controls important genes related to OA, including matrix metalloproteinase 9 and IL8, suggesting that it is a key factor in OA [9]. Lan L's study further supported the function of Notch signaling in the development of temporomandibular joint OA [45]. The study showed that in the state of temporomandibular joint OA, the expression of Notch1, Jagged1, and Hes5 increased over time, while the expression of Hes1 was initially inhibited and then upregulated.

Additionally, the Notch signaling pathway is essential for regulating macrophage polarization and related cellular processes. Qi *et al.* observed that the E3 ubiquitin ligase ITCH alleviated LPS-induced chondrocyte damage by degrading *JAG1* through K48 ubiquitination, thereby inhibiting Notch1 activation, reducing apoptosis and inflammation, and protecting the extracellular matrix [10]. Chen *et al.* emphasized that Notch activation promotes M1 macrophage polarization and enhances inflammation and anti-tumor activity, while inhibition transforms macrophages to M2 phenotype, suppresses inflammation, and promotes tumor progression [12]. Similarly, research by Hans *et al.* revealed that Notch1 haploinsufficiency enhances M2 polarization through TGF-β signaling and extracellular matrix remodeling [13]. In addition, Pagie *et al.* reported that *DLL4*-activated Notch signaling inhibits M2 polarization by inhibiting IL-4-induced markers and inducing caspase-dependent apoptosis, selectively *regulating Notch1, JAG1,* and pro-apoptotic pathways to disrupt M2 differentiation and favor M1 polarization [46]. In our study, *JAG1* activated the Notch signaling pathway in the OA model, and knockdown of *JAG1* significantly reduced the manifestation of Notch-related genes. In addition, *JAG1* promoted M1 macrophage polarization by regulating Notch signaling, and overexpression reversed the effects of *JAG1* knockdown and affected OA-related inflammation. These findings together emphasize the crucial role of Notch signaling in the occurrence and development of OA and TMJOA.

Despite the novel findings of this study, several limitations should be acknowledged. First, all experiments were conducted *in vitro* using a simplified model, which cannot fully replicate the complexity of the synovial microenvironment *in vivo*, such as the influence of other resident or infiltrating cell types (e.g., T cells, endothelial cells) and biomechanical stress. Second, although we observed that *JAG1* silencing reduced the expression of downstream Notch pathway targets (*Hes1*, *Hes5*, *Hey1*, and *Hey2*), these measurements were obtained from FLSs cultured independently under OA-like stimulation, rather than directly from SMs or co-culture systems. Thus, while the data

suggest that *JAG1* activates the Notch pathway in FLSs, further studies are needed to determine whether Notch signaling is similarly activated in SMs. This could be addressed by detecting NICD protein levels or *Hes*/*Hey* gene expression directly in SMs after co-culture.

In addition, while JAG1/Notch signaling is highlighted as a potential therapeutic target, the translational feasibility remains to be clarified. Several JAG1- or Notch-targeting agents, including monoclonal antibodies and γ-secretase inhibitors, are under investigation for oncology and immune-related conditions; however, their therapeutic effects and safety profiles in OA remain unknown. Future studies using *in vivo* OA models, including *JAG1*-deficient mice or Notch pathway inhibitors, are warranted to test the therapeutic potential of targeting this axis in joint disease.

Moreover, although multiple public datasets were analyzed, the total sample size remains relatively small, and experimental validation was limited to *in vitro* studies. Increasing the number of independent biological replicates and including clinical specimens or animal models in future work would enhance the robustness and generalizability of the findings.

Lastly, although this study focused on the Notch signaling pathway, other inflammatory or metabolic pathways – such as NF-κB and PI3K/Akt – are also known to regulate macrophage polarization and may be involved in JAG1-mediated effects. Further mechanistic investigations are needed to clarify the crosstalk between these pathways and *JAG1* in the context of OA. Overall, future research should integrate *in vivo* validation, pathway-specific assays in macrophages, and clinical correlation analyses to more fully evaluate the potential of *JAG1* as a therapeutic target in OA.

In conclusion, this study highlights the role of *JAG1* in OA through its activation of the Notch signaling pathway. Our results demonstrate that *JAG1* influences the polarization of SMs, promoting a shift toward the M1 phenotype, which is associated with inflammation. Knockdown of *JAG1* significantly decreased the expression of genes related to the Notch pathway, whereas overexpression of *JAG1* reversed these effects. These findings suggest that *JAG1* may influence the inflammatory microenvironment in OA by regulating macrophage polarization, providing preliminary evidence for its potential as a therapeutic target in controlling inflammation and tissue remodeling in OA.

Availability of data and materials

The datasets used and/or analyzed during the current study are available from the corresponding author upon reasonable request.

Funding

No external funding.

Ethical approval

Not applicable.

Conflict of interest

The authors declare no conflict of interest.

References

1. Terkawi MA, Ebata T, Yokota S, et al. Low-grade inflammation in the pathogenesis of osteoarthritis: cellular and molecular mechanisms and strategies for future therapeutic intervention. Biomedicines 2022; 10: 1109.
2. Cui L, Han Y, Dong Z. miR-106a mimics the nuclear factor-κB signalling pathway by targeting DR6 in rats with osteoarthritis. Arch Med Sci 2024; 20: 302-8.
3. Jrad AIS, Trad M, Bzeih W, El Hasbani G, Uthman I. Role of pro-inflammatory interleukins in osteoarthritis: a narrative review. Connect Tissue Res 2023; 64: 238-47.
4. Maglaviceanu A, Wu B, Kapoor M. Fibroblast-like synoviocytes: role in synovial fibrosis associated with osteoarthritis. Wound Repair Regen 2021; 29: 642-9.
5. Waszczykowski M, Fabiś-Strobin A, Bednarski I, Narbutt J, Fabiś J. Serum and synovial fluid concentrations of interleukin-18 and interleukin-20 in patients with osteoarthritis of the knee and their correlation with other markers of inflammation and turnover of joint cartilage. Arch Med Sci 2022; 18: 448-58.
6. Damerau A, Rosenow E, Alkhoury D, Buttgereit F, Gaber T. Fibrotic pathways and fibroblast-like synoviocyte phenotypes in osteoarthritis. Front Immunol 2024; 15: 1385006.
7. Panizo S, Martínez-Arias L, Alonso-Montes C, et al. Fibrosis in chronic kidney disease: pathogenesis and consequences. Int J Mol Sci 2021; 22: 408.
8. Vázquez-Ulloa E, Lin KL, Lizano M, Sahlgren C. Reversible and bidirectional signaling of notch ligands. Crit Rev Biochem Mol Biol 2022; 57: 377-98.
9. Karlsson C, Brantsing C, Egell S, Lindahl A. Notch1, Jagged1, and HES5 are abundantly expressed in osteoarthritis. Cells Tissues Organs 2008; 188: 287-98.
10. Qi L, Wang M, He J, Jia B, Ren J, Zheng S. E3 ubiquitin ligase ITCH improves LPS-induced chondrocyte injury by mediating JAG1 ubiquitination in osteoarthritis. Chemicobiol Interact 2022; 360: 109921.
11. Zhang H, Lin C, Zeng C, et al. Synovial macrophage M1 polarisation exacerbates experimental osteoarthritis partially through R-spondin-2. Ann Rheum Dis 2018; 77: 1524-34.
12. Chen W, Liu Y, Chen J, et al. The Notch signaling pathway regulates macrophage polarization in liver diseases. Int Immunopharmacol 2021; 99: 107938.
13. Hans CP, Sharma N, Sen S, et al. Transcriptomics analysis reveals new insights into the roles of Notch1 signaling on macrophage polarization. Sci Rep 2019; 9: 7999.
14. Liu J, Luo R, Zhang Y, Li X. Current status and perspective on molecular targets and therapeutic intervention strategy in hepatic ischemia-reperfusion injury. Clin Mol Hepatol 2024; 30: 585-619.
15. Condorelli AG, El Hachem M, Zambruno G, Nystrom A, Candi E, Castiglia D. Notch-ing up knowledge on molecular mechanisms of skin fibrosis: focus on the mul-

tifaceted Notch signalling pathway. J Biomed Sci 2021; 28: 36.
16. Breikaa R. Investigating the Role of Endothelial Cell-Expressed Jag1 On Smooth Muscle Function And Vascular Homeostasis. The Ohio State University 2022.
17. Xiao X, Wang W, Guo C, et al. Hypermethylation leads to the loss of HOXA5, resulting in JAG1 expression and NOTCH signaling contributing to kidney fibrosis. Kidney Int 2024; 106: 98-114.
18. Li X, Li Y, Zhang W, Jet al. The IGF2BP3/Notch/Jag1 pathway: a key regulator of hepatic stellate cell ferroptosis in liver fibrosis. Clin Transl Med 2024; 14: e1793.
19. Smyth GK. Linear models and empirical bayes methods for assessing differential expression in microarray experiments. Stat Appl Genet Mol Biol 2004; 3: 3.
20. Szklarczyk D, Kirsch R, Koutrouli M, et al. The STRING database in 2023: protein-protein association networks and functional enrichment analyses for any sequenced genome of interest. Nucleic Acids Res 2023; 51: D638-46.
21. Shannon P, Markiel A, Ozier O, et al. Cytoscape: a software environment for integrated models of biomolecular interaction networks. Genome Res 2003; 13: 2498-504.
22. Liu B, Xian Y, Chen X, et al. Inflammatory fibroblast-like synoviocyte-derived exosomes aggravate osteoarthritis via enhancing macrophage glycolysis. Adv Sci 2024; 11: e2307338.
23. Dakin SG, Buckley CD, Al-Mossawi MH, et al. Persistent stromal fibroblast activation is present in chronic tendinopathy. Arthritis Res Ther 2017; 19: 16.
24. Arunachalam K, Sasidharan SP, Arunachalam K, Sasidharan SP. Protein extraction and western blot analysis. Bioassays Exp Preclin Pharmacol 2021; 229-40.
25. Molnar V, Matišić V, Kodvanj I, et al. Cytokines and chemokines involved in osteoarthritis pathogenesis. Int J Mol Sci 2021; 22: 9208.
26. Gonzalez-Molina J, Moyano-Galceran L, Single A, et al. Chemotherapy as a regulator of extracellular matrix-cell communication: implications in therapy resistance. Semin Cancer Biol 2022; 86: 224-36.
27. Zhang S, Wang P, Hu B, et al. Inhibiting heat shock protein 90 attenuates nucleus pulposus fibrosis and pathologic angiogenesis induced by macrophages via down-regulating cell migration–inducing protein. Am J Pathol 2023; 193: 960-76.
28. Boutilier AJ, Elsawa SF. Macrophage polarization states in the tumor microenvironment. Int J Mol Sci 2021; 22: 6995.
29. Motta F, Barone E, Sica A, Selmi C. Inflammaging and osteoarthritis. Clin Rev Allergy Immunol 2023; 64: 222-38.
30. Jiang F, Zhao H, Zhang P, et al. Challenges in tendon–bone healing: emphasizing inflammatory modulation mechanisms and treatment. Front Endocrinol 2024; 15: 1485876.
31. Zhong Y, Wei B, Wang W, et al. Single-cell RNA-sequencing identifies bone marrow-derived progenitor cells as a main source of extracellular matrix-producing cells across multiple organ-based fibrotic diseases. Int J Biol Sci 2024; 20: 5027.
32. Ačkar L, Casjens S, Andreas A, et al. Blood-based detection of lung cancer using cysteine-rich angiogenic inducer 61 (CYR61) as a circulating protein biomarker: a pilot study. Mol Oncol 2021; 15: 2877-90.
33. Stone AV, Loeser RF, Vanderman KS, Long DL, Clark SC, Ferguson CM. Pro-inflammatory stimulation of meniscus cells increases production of matrix metalloproteinases and additional catabolic factors involved in osteoarthritis pathogenesis. Osteoarthritis Cartilage 2014; 22: 264-74.
34. Deroyer C, Poulet C, Paulissen G, et al. CEMIP (KIAA1199) regulates inflammation, hyperplasia and fibrosis in osteoarthritis synovial membrane. Cell Mol Life Sci 2022; 79: 260.
35. Maldonado M, Nam J. The role of changes in extracellular matrix of cartilage in the presence of inflammation on the pathology of osteoarthritis. BioMed Res Int 2013; 2013: 284873.
36. Kurowska-Stolarska M, Alivernini S. Synovial tissue macrophages in joint homeostasis, rheumatoid arthritis and disease remission. Nat Rev Rheumatol 2022; 18: 384-97.
37. Apeku E, Tantuoyir MM, Zheng R, Tanye N. Exploring the polarization of M1 and M2 macrophages in the context of skin diseases. Mol Biol Rep 2024; 51: 269.
38. Mao J, Chen L, Cai Z, et al. Advanced biomaterials for regulating polarization of macrophages in wound healing. Adv Funct Materials 2022; 32: 2111003.
39. Wang L, He C. Nrf2-mediated anti-inflammatory polarization of macrophages as therapeutic targets for osteoarthritis. Front Immunol 2022; 13: 967193.
40. Fang C, Zhong R, Lu S, et al. TREM2 promotes macrophage polarization from M1 to M2 and suppresses osteoarthritis through the NF-κB/CXCL3 axis. Int J Biol Sci 2024; 20: 1992.
41. Anusewicz D, Orzechowska M, Bednarek AK. Notch signaling pathway in cancer – review with bioinformatic analysis. Cancers 2021; 13: 768.
42. Ng C, Qin Y, Xia Y, Hu X, Zhao B. Jagged1 acts as an RBP-J target and feedback suppresses TNF-mediated inflammatory osteoclastogenesis. J Immunol 2023; 211: 1340-7.
43. Zack SR, Meyer A, Zanotti B, et al. Notch ligands are biomarkers of anti-TNF response in RA patients. Angiogenesis 2024; 27: 273-83.
44. Lin NY, Distler A, Beyer C, et al. Inhibition of Notch1 promotes hedgehog signalling in a HES1-dependent manner in chondrocytes and exacerbates experimental osteoarthritis. Ann Rheum Dis 2016; 75: 2037-44.
45. Lan L, Jiang Y, Zhang W, Li T, Ying B, Zhu S. Expression of Notch signaling pathway during osteoarthritis in the temporomandibular joint. J Craniomaxillofac Surg 2017; 45: 1338-48.
46. Pagie S, Gérard N, Charreau B. Notch signaling triggered via the ligand DLL4 impedes M2 macrophage differentiation and promotes their apoptosis. Cell Commun Signal 2018; 16: 4.